Glutamate receptor-channel gating

Maximum likelihood analysis of gigaohm seal recordings from locust muscle

S. E. Bates,* M. S. P. Sansom,* F. G. Ball,‡ R. L. Ramsey,* and P. N. R. Usherwood*

*Department of Zoology, and ‡Department of Mathematics, University of Nottingham, University Park, Nottingham, NG7 2RD, United Kingdom

ABSTRACT Gigaohm recordings have been made from glutamate receptor channels in excised, outside-out patches of collagenase-treated locust muscle membrane. The channels in the excised patches exhibit the kinetic state switching first seen in megaohm recordings from intact muscle fibers. Analysis of channel dwell time distributions reveals that the gating mechanism contains at least four open states and at least four closed states. Dwell time autocorrelation function analysis shows that there are at least three gateways linking the open states of the channel with the closed states. A maximum likelihood procedure has been used to fit six different gating models to the single channel data. Of these models, a cooperative model yields the best fit, and accurately predicts most features of the observed channel gating kinetics.

INTRODUCTION

Single channel recording has been used to explore the properties of the quisqualate-sensitive glutamate receptor-channel (qGluR) of locust muscle (Patlak et al., 1979; Gration et al., 1981*a* and *b*, 1982) and to gain an understanding of the molecular mechanisms underlying the gating kinetics of this receptor (Kerry et al., 1987, 1988). So far, our kinetic modeling of qGluR channel data has been limited to fitting possible gating models to single channel dose-response curves. More sophisticated modeling is required to give estimates of all kinetic parameters for a particular gating model, and to allow comparison of the goodness-of-fit of alternative models to the experimental data. Although our physiological studies, hitherto, have employed a megaohm recording configuration in which pretreatment of the muscle membrane with collagenase and other proteases is avoided, the resultant noise levels in the single channel recordings are such that brief openings and closings (shorter than a minimum dwell time of 0.2 ms) are incompletely resolved. In this paper we describe the application of a gigaohm recording technique to locust qGluR in which, as previously, we have used concanavalin A to inhibit qGluR desensitization (Mathers and Usherwood, 1976; Evans and Usherwood, 1985), thereby enabling one to focus on channel activation by binding of L-glutamate to the receptor. Preliminary modeling of the qGluR gating kinetics using the maximum likelihood procedure of Ball and Sansom (1989) is also described. An account of part of this work has appeared in abstract form (Bates et al., 1988; Sansom et al., 1989*a*).

METHODS

Experimental

Extensor tibiae muscles of the metathoracic legs of adult female locusts (*Schistocerca gregaria*) were dissected in 180 mM NaCl, 10 mM KCl, 2 mM $CaCl_2$, 3 mM Hepes, pH 6.8. The muscles were incubated in collagenase (2 mg/ml, type IA, Sigma Chemical Co., St. Louis, MO) for 1.5–2 h at 27–30°C before use. All subsequent procedures were undertaken at room temperature (~20°C).

During recordings, both patch pipette and bath contained 19 mM NaCl, 86 mM Na_2SO_4, 3 mM Hepes, pH 6.8. Use of these salines almost completely suppressed K^+ and Cl^- channel activity. Patch electrodes (5–10 MΩ resistance) were used to obtain excised, outside-out membrane patches. These patches were first exposed to concanavalin A (1–2 μM, for 1–6 min) to block desensitization, and subsequently perfused with L-glutamate. The entire procedure was undertaken in the flow cell depicted in Fig. 1. Single channel currents were recorded using a model EPC7 amplifier (Adams and List Associates, Great Neck, NY), and stored on video tape using a Sony PCM701 and a Betamax VCR.

Computational

Computer analysis was performed on a Masscomp MC5500 (Concurrent Computer Corporation Ltd., Berkshire, England) equipped with a floating point processor. Data acquisition and reduction programs were written in C; data analysis and modeling programs were written in Fortran77. The NAG library was used as a source of numerical subroutines.

Single channel recordings were low-pass filtered at 10 kHz on playback, and digitized at a sampling frequency of 50 kHz. Data reduction was achieved using a half amplitude threshold crossing algorithm. The reduced data consisted of a vector of channel open and closed times. These vectors were employed in all subsequent kinetic analysis. Each patch was tested over a range of L-glutamate concentrations, and only those patches which did not exhibit more than one open channel conductance level at high concentrations were analyzed. It was assumed that this procedure restricted our analysis to single qGluR.

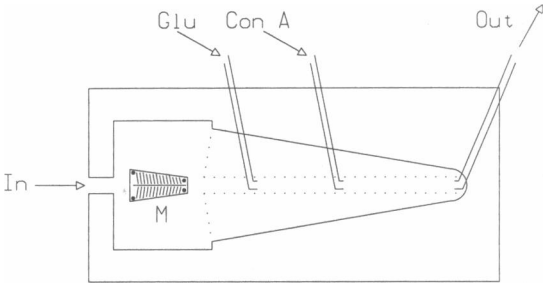

FIGURE 1 Diagram of the flow cell used for gigaohm recordings from excised, outside-out patches of locust muscle membrane. The dissected muscle (*M*) is depicted on the left of the diagram. After formation, an excised patch is moved to the right hand capillary (*Con A*) and exposed to lectin, before being moved to the left hand capillary (*Glu*) for exposure to L-glutamate. A constant flow of saline through the bath is maintained via the inlet and outlet as depicted.

Open and closed (dwell) time distributions were constructed using log binning and displayed on log–log plots (McManus et al., 1987; Kerry et al., 1988; Sansom et al., 1989*b*). Multiexponential probability density functions were fitted to the dwell time distributions using the method described by Sansom et al. (1989*b*). Alternative fits to the dwell time distributions were discriminated between using a bootstrap procedure (Efron, 1983; Horn, 1987; Sansom et al., 1989*b*). Channel dwell time autocorrelation functions were evaluated and fitted as described in our earlier publications (Kerry et al., 1987, 1988). A maximum likelihood procedure was used to fit gating models to channel data. The method allowed a gating model to be fitted simultaneously to multiple channel dwell time vectors derived from separate patch clamp experiments. This approach was pioneered by Horn and Lange (1983). Details of the algorithm employed in our investigations are given in Ball and Sansom (1989). Simulation of single channel currents was performed using the procedures described by, for example, Clay and DeFelice (1983).

RESULTS

Gigaohm qGluR recordings

Channel currents in response to application of L-glutamate (10^{-5} to 10^{-2} M) were obtained in ~10% of the patches after concanavalin A treatment. The majority of these did not exhibit desensitization kinetics. Exposure of the excised, outside-out patches to concanavalin A clearly blocked qGluR desensitization. For example, in the presence of a high (10^{-2} M) concentration of glutamate, continuous channel activity could be observed. If desensitization had still been present, little or no channel activity would have been expected under such conditions. The single channel conductance was ~150 pS, i.e., close to that of the qGluR channel recorded in megaohm experiments. The signal to noise ratio in the gigaohm records was ~4:1 at a low-pass filter cutoff of 10 kHz. This was clearly superior to the signal-to-noise ratio of 3:1 which was obtained after filtering megaohm records at 3 kHz (Kerry et al., 1987). As in the megaohm experiments, usually only a single main conductance level was present in the recordings, and only recordings containing activity from a single qGluR were analyzed (see Methods).

The level of channel activity was dependent upon the concentration of glutamate with which the patch was perfused (Fig. 2). With 10^{-5} M L-glutamate only occasional, brief channel openings were seen, whereas with 10^{-2} M L-glutamate the qGluR channel spent most of its time open. The kinetic state switching first observed in the megaohm system by Patlak et al. (1979) was also seen in the gigaohm recordings. Thus, in the presence of 10^{-3} M L-glutamate (Fig. 2) three general modes of channel activity were observed: (I) channel predominantly closed; (II) channel closed with numerous brief openings; and (III) channel open with numerous brief closings. In a minority of patches brief channel openings were obtained at high L-glutamate concentrations, reminiscent of those observed by Dudel et al. (1988) (S channel). These patches were discarded.

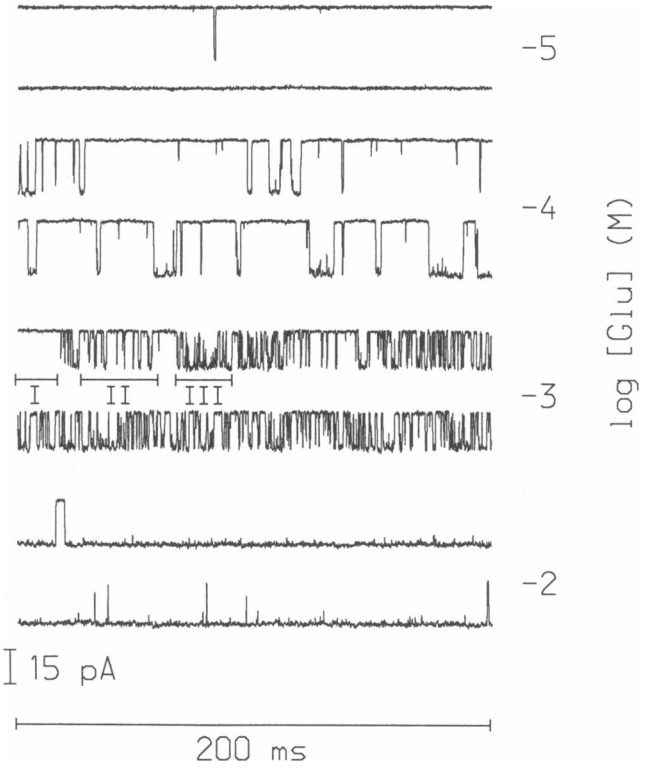

FIGURE 2 Representative single qGluR channel recordings in response to four concentrations of L-glutamate. The three gating modes (I–III) discussed in the text are marked on the recording made in the presence of 10^{-3} M L-glutamate.

TABLE 1 Summary of gigaohm database

[Glu]	N_{evt}	m_o	m_c	T_{tot}
m		*ms*	*ms*	*s*
1.0×10^{-5}	117	0.11	621.0	72.7
1.0×10^{-4}	957	0.34	38.1	36.8
5.0×10^{-4}	15517	0.43	26.3	414.0
1.0×10^{-3}	23014	9.56	2.55	279.0
1.0×10^{-2}	1006	56.7	20.8	78.0

N_{evt} is the number of events (where one event is defined as an opening plus the following closing) in the data set. The mean open and mean closed times are m_o and m_c, respectively, and T_{tot} is the total duration of the combined recordings for a given L-glutamate concentration ([Glu]).

Dose-response relationships

Single channel recordings were obtained over a range of L-glutamate concentrations (Table 1). The database employed for kinetic analysis consisted of 40, 611 channel openings, obtained from nine membrane patches, over an L-glutamate concentration range of 10^{-5} to 10^{-2} M. The mean open time (m_o) of the channel rises from ~0.1 ms with 10^{-5} M to ~60 ms with 10^{-2} M L-glutamate. The mean closed time (m_o) falls with increasing L-glutamate concentration until it reaches a minimum with 10^{-3} M. It then rises again slightly during application of higher concentrations of agonist. These relationships of mean dwell times to agonist concentration parallel those revealed by our previous analysis of megaohm data obtained from qGluR (Kerry et al., 1987, 1988).

Hill plot analysis of the relationship between channel open probability (P_o) and L-glutamate concentration (Fig. 3) gave a Hill coefficient of $n_H = 1.5$. The apparent dissociation constant was $K_D = 1.45 \times 10^{-4}$ M. The Hill coefficient is comparable with that obtained from the megaohm data (1.6; Kerry et al., 1988), but the K_D is about 10-fold higher.

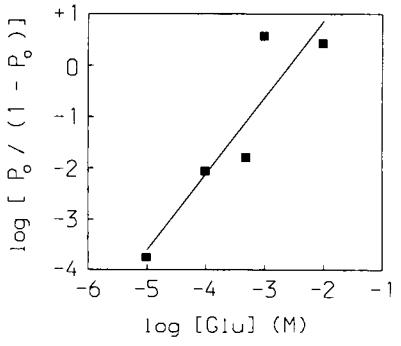

FIGURE 3 Hill plot derived from the L-glutamate concentration ([*Glu*]) dependence of the channel open probability (P_o). The fitted line corresponds to $\log [P_o/(1 - P_o)] = n_H \log [Glu] - \log K_D$ with $n_H = 1.5$ and $K_D = 1.45 \times 10^{-4}$ M.

Dwell time probability density functions

Analysis of open-time and closed-time distributions can be used to determine the numbers of open and closed states of the channel gating mechanism (Colquhoun and Hawkes, 1981, 1982; Horn, 1984; Fredkin et al., 1985). We present here the analysis of a long recording (12,612 channel openings) obtained using 10^{-3} M L-glutamate. Comparable results have been obtained from the other recordings. Both the open- and closed-time distributions peaked at ~0.08 ms if all events were included in the analysis irrespective of duration. Thus the minimum fully-detectable, open-channel dwell time was 0.08 ms (~0.2 ms for megaohm data). In the presence of 10^{-3} M L-glutamate ($P_o = 0.70$) channel open times ranged from 0.08 to ~80 ms duration. The open-time distribution (Fig. 4 *A*) clearly could not be fitted by a single exponential function. A sum of three exponentials fitted all of the distribution except for the tail of long duration openings, the latter being fitted well only if four exponentials were used. The three- and four-exponential fits were compared using the bootstrap procedure (Horn, 1987; Sansom et al., 1989*b*). This involved randomly resampling (with replacement) the dwell time data so as to generate 50 equivalent resampled data sets. Each of the resampled data sets was used to produce an open-time distribution, and the distribution was fitted with three and with four exponentials. For each resampled data set, the SC predictor ratio, given by $P_{4/3} = SC_3 - SC_4$ where SC_3 and SC_4 are the Schwarz criteria for the three- and four-exponential fits, respectively, was calculated. Thus, 50 values of $P_{4/3}$ were generated and used to construct the corresponding histogram (Fig. 4 *B*). This was fitted with a normal distribution, and the mean and variance of the normal distribution used to estimate the probability that $P_{4/3} > 0$. This probability is a measure of the confidence that the four-exponential probability density function (PDF) provides a better fit to the open-time distribution than the three-exponential PDF. Such analysis of the qGluR open-time data yielded a figure of 0.933 for this probability. The time constants (τ_i) for the four components (Table 2) are relatively close; hence the absence of pronounced shoulders when the open-time distribution is displayed on log–log scales. The closed times ranged from 0.08 to ~300 ms. Again a four-component PDF gave the best fit to the observed distribution (Fig. 4 *C*). Bootstrap analysis showed that the probability of the four-component PDF providing a better fit than the three-component PDF was 0.999. The τ_i values for the closed-time PDF

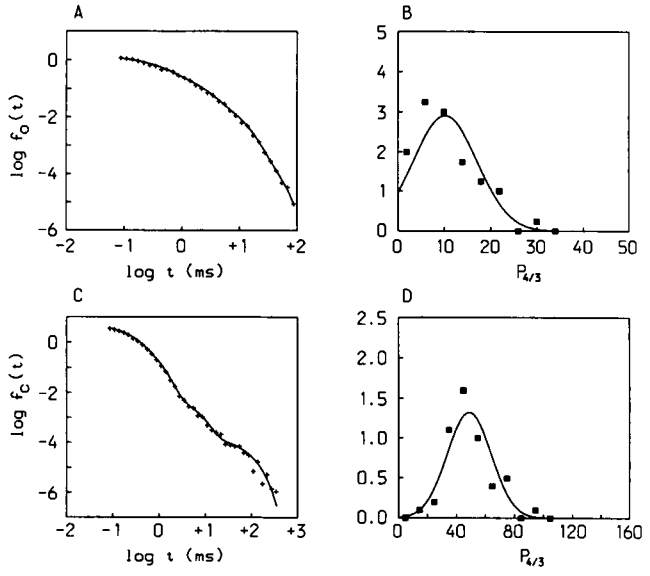

FIGURE 4 Analysis of channel dwell time distributions derived from recordings made in the presence of 10^{-3} M L-glutamate. (*A*) Open time distribution (+) displayed on log–log scales with a four-exponential fit (Table 2) superimposed. (*B*) Result of bootstrap analysis to compare four- and three-exponential fits to the open-time distribution. Points represent the distribution of SC predictor ratios ($P_{4/3}$) for comparison of four- and three-exponential PDFs fitted to 50 bootstrap resampled datasets. The corresponding normal curve is superimposed. If the four- and three-exponential PDFs provided equally satisfactory descriptions of the experimental data, then the $P_{4/3}$ distribution would be centered about zero. It is clearly centered about a value greater than zero, indicating that the four-exponential fit is significantly better than the three-exponential fit. The closed time distribution (+) and its four-exponential fit (Table 2), and the corresponding $P_{4/3}$ distribution, are shown in *C* and *D*, respectively.

were sufficiently well separated (Table 2) for shoulders to be visible when the distribution is plotted on log–log scales (Fig. 4). Overall, analysis of dwell time PDFs suggests that the channel exists in at least four distinct closed states ($N_c \geq 4$) and at least four open states ($N_o \geq 4$). This degree of kinetic complexity is the same as that observed from analysis of megaohm recordings of locust muscle qGluR (Kerry et al., 1987, 1988).

TABLE 2 Open and closed time PDFs at [Glu] = 1×10^{-3} M

Open time PDF ($N_o = 4$)			Closed time PDF ($N_c = 4$)		
i	α_i	τ_i	i	α_i	τ_i
		ms			*ms*
1	0.27	0.31	1	0.58	0.18
2	0.45	1.4	2	0.38	0.49
3	0.26	5.4	3	0.03	3.8
4	0.02	17	4	0.01	56

Both PDFs were fitted using $f(t) = \Sigma_{i=1}^{4} (\alpha_i/\tau_i) \exp(-t/\tau_i) / \Sigma_{i=1}^{4} \alpha_i [\exp(-t_{min}/\tau_i) - \exp(-t_{max}/\tau_i)]$, where t_{min} is the minimum dwell time and t_{max} the maximum dwell time used to estimate the dwell time distribution.

Dwell time autocorrelation functions

Analysis of correlations between successive open and successive closed times indicates the number of *gateway* states of a channel gating mechanism (Fredkin et al., 1985; McManus et al., 1985; Labarca et al., 1985; Colquhoun and Hawkes, 1987; Kerry et al., 1987, 1988; Ball and Sansom, 1988; Ball and Rice, 1989; Blatz and Magleby, 1989). An *open gateway state* is defined as an open state from which the channel may enter the closed state aggregate. A closed gateway state is defined as a closed state from which the channel may enter the open state aggregate. Let N_g be the minimum of N_{go} and N_{gc}, where N_{go} is the number of open gateway states and N_{gc} is the number of closed gateway states. Assuming that the channel gating mechanism is at thermodynamic equilibrium, i.e., that the underlying Markov process is time reversible, the single-channel open time and closed time autocorrelation functions (ACFs) take the form of the sum of M geometric decays with positive coefficients. As shown by Fredkin et al. (1985), M is determined by N_g, specifically $M \leq N_g - 1$. Thus evaluation and fitting of dwell time ACFs provides a way of estimating the number of gateway states of the channel. For example, mechanism I in Fig. 5 has $N_g = 1$ and hence would not result in correlations between successive dwell times. By contrast, mechanism II has $N_g = 2$, which would result in positive ACFs best fitted by a single geometric decay.

Positive autocorrelations were observed for all long recordings of qGluR subjected to ACF analysis. The ACFs obtained from analysis of a 13,097-event-long recording obtained in the presence of 5×10^{-4} M L-glutamate is shown in Fig. 6. Positive ACFs are clearly present, both for channel openings (Fig. 6 *A*) and for channel closings (Fig. 6 *B*). The open time ACF was fitted with a single geometric decay; the closed time ACF with the sum of two such decays (Table 3). On the basis of this analysis we may conclude that $N_g \geq 3$, and that hence the underlying gating mechanism is either branched or cyclic. We arrived at a similar conclusion after ACF analysis of megaohm data from locust muscle qGluR (Kerry et al., 1987, 1988).

Modeling

The maximum likelihood procedure (Ball and Sansom, 1989) was used to fit six different gating models to the gigaohm qGluR database summarized in Table 1. Models

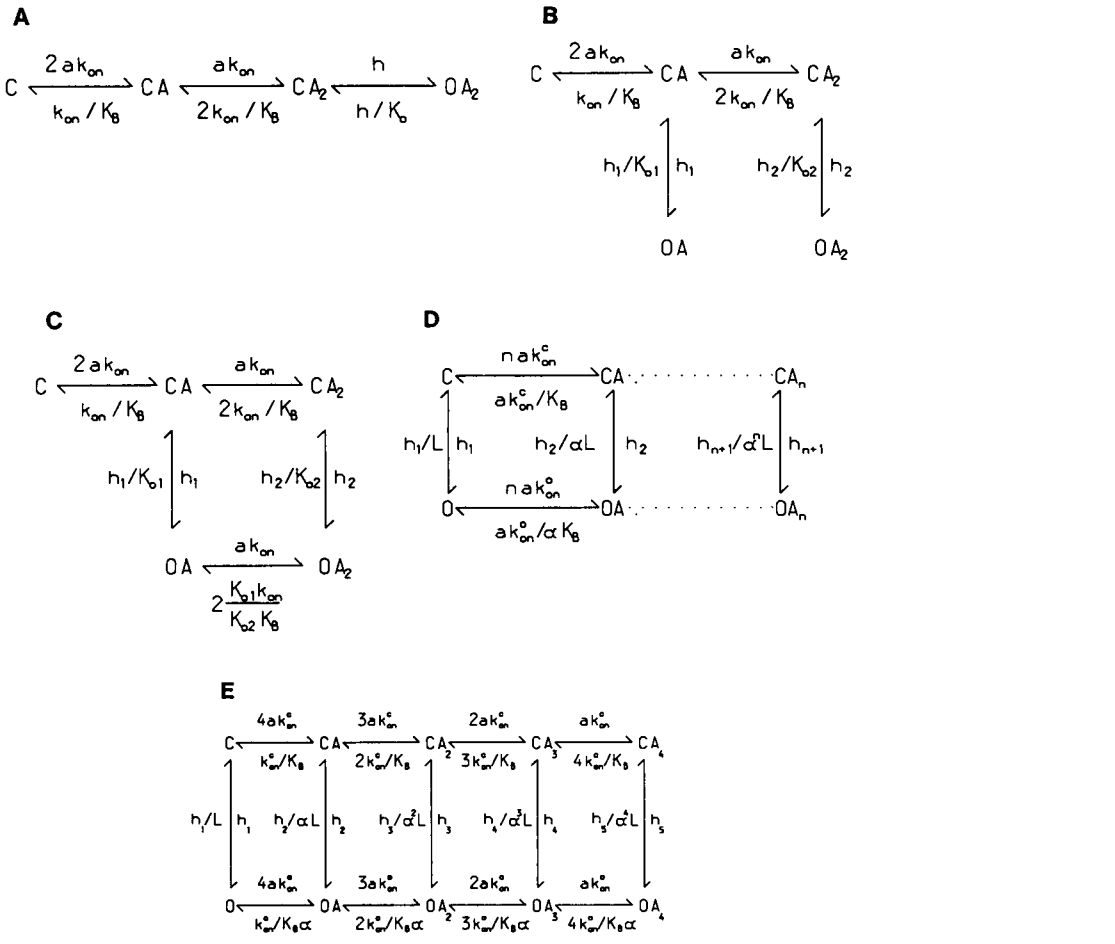

FIGURE 5 Gating models fitted to gigaohm qGluR data using the maximum likelihood procedure. *C* represents the closed receptor channel, *O* the open receptor channel, and *A* the agonist (L-glutamate) molecule. Models I–III (see text) are shown in *A*, *B*, and *C*, respectively. Cooperative (C-*n*) models are illustrated in *D*. The C-4 model is defined in full in *E*. Further discussions of these models is provided in the text.

I–III have all been used to model the kinetics of the nicotinic acetylcholine receptor. Model I has recently been used in two sets of studies of the nicotinic acetylcholine receptor (nAChR) which related channel activation to the agonist employed (Ogden et al., 1987; Papke et al., 1988). It is assumed that there are two equivalent agonist binding sites, and that the channel may only open once both agonist molecules have bound. The model is characterized by two equilibrium constants, the agonist binding constant K_B and the equilibrium constant for opening of the (biliganded) channel K_O, and by two kinetic constants, the agonist binding rate k_{on} and the opening rate of the channel h. Model II has been used, for example, by Labarca et al. (1985) to explain the gating kinetics of reconstituted *Torpedo* nAChR. It is essentially a modification of model I, in which openings of the monoliganded receptor channel are permitted, but are briefer than openings of the biliganded receptor. The two binding sites are assumed to have the same microscopic affinity and binding rates for the agonist, but the closed-open equilibrium constants (K_{O_1} and K_{O_2}) and the opening rates (h_1 and h_2) of the monoliganded and biliganded states, respectively, are assumed to be different. Model III is a further modification of model I in which the second agonist molecule may bind after the monoliganded channel has opened. It has been employed e.g. by Colquhoun and Sakmann (1985) to interpret the fast kinetics of the frog muscle nAChR. There are no parameters additional to those for model II, as it has been assumed that (*a*) the agonist binding rate is independent of whether the channel is open or closed and (*b*) the cycle is at thermodynamic equilibrium. We have evidence that the latter assumption is justified in the case of the qGluR in that (*a*) dwell time cross-correlation analysis of megaohm qGluR data indicates that the channel gating mechanism is at equilibrium (Ball et al., 1988) and (*b*) positive ACFs (see

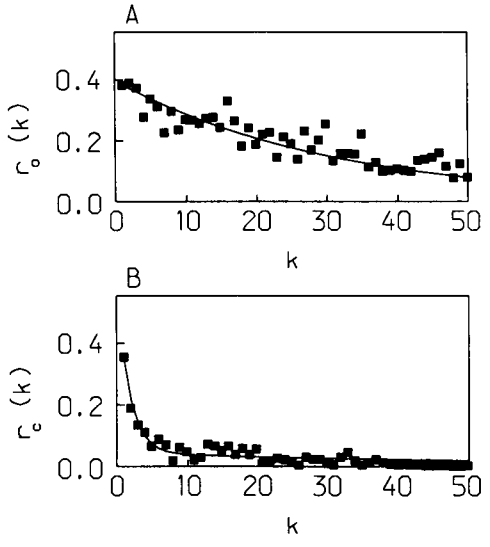

FIGURE 6 Autocorrelation functions for successive open (*A*) and closed (*B*) times derived from recordings made in the presence of 5 × 10^{-4} M L-glutamate. The points represent the estimated ACFs, the curves the corresponding fits (see Table 3).

above) are consistent with an equilibrium gating mechanism (Ball and Rice, 1989).

The other three models (C-2 to C-4) are based on the cooperative model for protein allosteric effects (Monod et al., 1965), which was first applied to the nAChR by Karlin (1967). We have employed this class of model in our previous studies of qGluR gating (Kerry et al., 1988). The basic tenets of this model are: (*a*) the channel protein can exist in two conformations, open or closed; (*b*) there are n identical agonist binding sites on the receptor-channel complex; and (*c*) when the channel is open the microscopic affinity of the agonist binding sites is increased. If there are n binding sites then the C-n model (as formulated in Fig. 5) is defined by $n + 6$ independent parameters. There are three equilibrium parameters: the agonist binding constant for the closed channel K_B, the ratio of the agonist binding constant for the open channel to that for the closed channel α, and the closed-to-open equilibrium constant for the unliganded receptor channel complex L. There are two agonist binding rates: for the closed receptor-channel k_{on}^{c} and for the open k_{on}^{o}. Finally, there are $n + 1$ channel opening rates, corresponding to the $n + 1$ different numbers of agonist molecules (0 to n) which may be bound. Thus the C-4 model is defined by 10 independent parameters: K_B, α, L, k_{on}^{c}, k_{on}^{o}, and the channel opening rates h_i, $i = 1$–5. These parameters can be used to calculate all 26 of the rate constants in the C-4 model (Fig. 5 *E*).

TABLE 3 Open and closed time ACFs at [Glu] = 5 × 10^{-4} M

Open time ACF ($N_g - 1 = 1$)			Closed time ACF ($N_g - 1 = 2$)		
i	A_i	π_i	i	A_i	π_i
1	0.396	0.968	1	0.53	0.57
			2	0.05	0.95

The ACFs were fitted by: $r(k) = \Sigma_{i=1}^{N_g-1} A_i \pi_i^k$, i.e., by the sum of $N_g - 1$ geometrically decaying terms.

At this point it is valuable to consider what is the maximum number of independent parameters which a model may have if it is to be identifiable on the basis of single channel data. Fredkin et al. (1985) have pointed out that models with more than $2N_oN_c$ free parameters cannot be identified by analysis of single channel data. If one assumes time reversibility for the gating mechanism (i.e., if the mechanism is at thermodynamic equilibrium) then the maximum number of free parameters is reduced to $N_oN_c + N_o + N_c - 1$ (see Appendix). From the gigaohm data we have estimated that $N_o = N_c = 4$ and hence we estimate that models with up to 23 independent parameters may be identifiable.

All six models were fitted to the database of 40,000 channel events. The CPU times for fitting ranged from ~20 min for model I to ~4 d for model C-4. The CPU time required to evaluate the likelihood for a single point in parameter space was shown empirically to vary approximately in proportion to $10^{0.35N}$ where N was the number of parameters in the model. The parameter estimates for the fitted models are listed in Table 4. The agonist dissociation constants ($1/K_B$) range from 1.5 × 10^{-3} M for model I to 9.3 × 10^{-3} M for model C-3. The agonist binding rates range from 110 M^{-1} ms^{-1} for model I to 3.2 M^{-1} ms^{-1} for model C-2. These are all less than the diffusion-limited rate of binding of *c.* 10^4 $M^{-1}ms^{-1}$, but the ranges of values are consistent with those arrived at for the C-4 model on the basis of less formal modeling of our megaohm data (Kerry et al., 1988).

The model fits were ranked on the basis of the Schwarz criterion (*SC*; Schwarz, 1978) as discussed by Ball and Sansom (1989). The *SC* is given by

$$SC = -\hat{L} + \tfrac{1}{2}N \ln M,$$

where $\hat{L}$ is the maximum likelihood, N is the number of parameters in the model, and M is the number of observations. The "best" model is that with the lowest *SC*. The resultant ranking (Table 5) suggests that, of the models tested, C-4 gives the best fit to the data. Whereas this does not demonstrate C-4 is a definitive model for qGluR, it does provide a working hypothesis worthy of more detailed examination.

TABLE 4 Parameter estimates for gating models

		Model I		
$K_B = 660\ M^{-1}$	$K_O = 10$			
$k_{on} = 110\ M^{-1}ms^{-1}$	$h = 1.5\ ms^{-1}$			
		Model II		
$K_B = 110\ M^{-1}$	$K_{O_1} = 0.30$	$K_{O_2} = 52$		
$k_{on} = 17\ M^{-1}ms^{-1}$	$h_1 = 0.61\ ms^{-1}$	$h_2 = 3.4\ ms^{-1}$		
		Model III		
$K_B = 130\ M^{-1}$	$K_{O_1} = 0.30$	$K_{O_2} = 62$		
$k_{on} = 18\ M^{-1}ms^{-1}$	$h_1 = 0.62\ ms^{-1}$	$h_2 = 3.7\ ms^{-1}$		
		Model C-2		
$K_B = 130\ M^{-1}$	$L = 2.8 \times 10^{-3}$	$\alpha = 190$		
$k_{on}^c = 3.2\ M^{-1}ms^{-1}$	$k_{on}^o = 76\ M^{-1}ms^{-1}$			
$h_1 = 1.1 \times 10^{-2}\ ms^{-1}$	$h_2 = 8.3\ ms^{-1}$	$h_3 = 4.2\ ms^{-1}$		
		Model C-3		
$K_B = 110\ M^{-1}$	$L = 1.2 \times 10^{-3}$	$\alpha = 84$		
$k_{on}^c = 6.9\ M^{-1}ms^{-1}$	$k_{on}^o = 130\ M^{-1}ms^{-1}$			
$h_1 = 6.5 \times 10^{-4}\ ms^{-1}$	$h_2 = 0.31\ ms^{-1}$	$h_3 = 3.2\ ms^{-1}$	$h_4 = 6.1 \times 10^{-3}ms^{-1}$	
		Model C-4		
$K_B = 270\ M^{-1}$	$L = 1.5 \times 10^{-4}$	$\alpha = 44$		
$k_{on}^c = 3.7\ M^{-1}ms^{-1}$	$k_{on}^o = 126\ M^{-1}ms^{-1}$			
$h_1 = 1.1 \times 10^{-4}\ ms^{-1}$	$h_2 = 3.2 \times 10^{-2}\ ms^{-1}$	$h_3 = 0.69\ ms^{-1}$	$h_4 = 3.9\ ms^{-1}$	$h_5 = 6.4 \times 10^{-3}\ ms^{-1}$

Comparison of C-4 model with observed qGluR gating kinetics

A comparison of the predicted and the observed single channel dose-response relationships was made first. Both P_o and channel event frequency, f, were examined as functions of L-glutamate concentration (Fig. 7 *A*). The agreement between the experimentally determined values for P_o and f and the model predictions was good. In particular, the C-4 model accomodates the fall in event frequency seen at high L-glutamate concentrations, with a maximum in the frequency curve at $\sim 10^{-3}$ M. Hill plot analysis of the predicted P_o data gave a slope of $n_H = 2.2$, i.e., somewhat higher than that ($n_H = 1.5$) estimated from the experimental data.

TABLE 5 Ranking of gating models

Model	N	$\hat{L}\ (10^5)$	*SC* ranking
I	4	−1.88	6
II	6	−1.34	4
III	6	−1.34	4
C-2	8	−1.29	3
C-3	9	−1.25	2
C-4	10	−1.20	1

N is the number of parameters in the model; $\hat{L}$ is the maximum likelihood. The *SC* ranking is explained in the text, with the "'best" model ranked as 1.

The C-4 model was also used to simulate single-channel openings over a range of L-glutamate concentrations (Fig. 7 *b*). Simulated "recordings" were similar in appearance to experimental traces. In both cases, simulated and experimental, channel openings were brief and infrequent with 10^{-5} M L-glutamate, whereas closings were infrequent with 10^{-2} M L-glutamate. Also, the simulated data showed state switching with 10^{-3} M L-glutamate, which is consistent with what is seen experimentally, i.e., the three modes (I, predominantly closed; II, closed with brief openings; and III, open with brief closings) seen experimentally are reproduced in the simulation.

Finally, 40,000 channel openings were simulated for a L-glutamate concentration of 5×10^{-4} M, and dwell time PDFs and ACFs evaluated (Fig. 8). Both the open and the closed time PDFs showed multiple exponential components (Fig. 8, *A* and *B*). The distributions derived from the simulated data superimposed precisely on the corresponding theoretical PDFs calculated using the method of Colquhoun and Hawkes (1981). This validates the procedures used in evaluation of dwell time distributions, both for simulated and for experimental data. The simulated distributions were fitted with sums of exponentials using

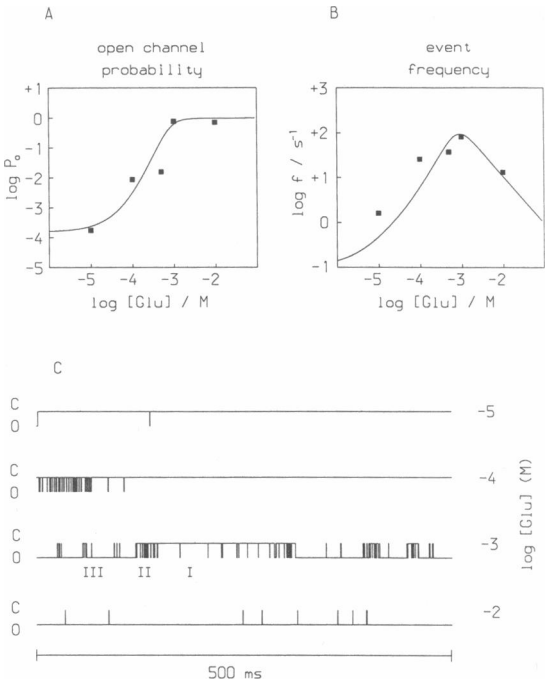

FIGURE 7 Predictions of channel behavior from the fitted C-4 model. In *A* and *B* the observed single-channel dose-response relationships (points) are compared with those predicted from the fitted C-4 model (curves). In *C* simulated single channel "recordings" for the C-4 model are shown (*C* = closed; *O* = open channel). These should be compared with the corresponding experimental recordings in Fig. 2.

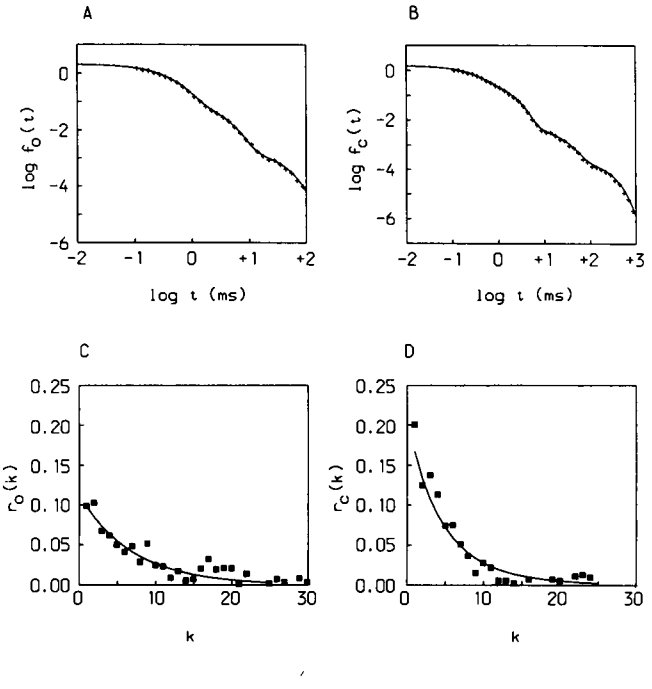

FIGURE 8 Kinetic analysis of simulated data for the C-4 model in the presence of 5×10^{-4} M L-glutamate. 40,000 channel openings were simulated. Brief channel openings (and closings) were not omitted from the simulated data. The open-time (*A*) and closed-time (*B*) distributions and the corresponding open-time (*C*) and closed-time (*D*) autocorrelation functions are shown. The results from the simulations are shown as points, superimposed upon the corresponding theoretical curves, which were evaluated as described by Colquhoun and Hawkes (1981; *A* and *B*) and by Ball and Sansom (1988; *C* and *D*).

the same procedures as those used for analysis of the experimental data. Best fits were obtained with $N_o = 3$ and $N_c = 4$. Thus a degree of kinetic complexity comparable with that arrived at from analysis of experimental data was observed. Positive ACFs (Fig. 8, *C* and *D*) were seen for both the open and for the closed times, although they were somewhat weaker than, and decayed more quickly than, those obtained from the experimental data.

DISCUSSION

qGluR channel kinetics in excised outside-out patches

We have shown that in outside-out patches excised from collagenase-treated locust muscle the single channel properties of the qGluR are similar to those observed in megaohm recordings. Desensitization can still be blocked by concanavalin A, which suggests that the lectin acts directly on the qGluR complex. If a cytoplasmic second messenger had mediated the concanavalin A effect, one would not expect to see block of desensitization when the lectin is applied to excised, outside-out patches. There remains the possibility that concanavalin A acts via a membrane-localized second messenger or via a direct G protein interaction or via binding to glycolipids to cause membrane stabilization, but in the absence of any further evidence we prefer the simpler explanation.

There is a decrease in the apparent affinity of qGluR for L-glutamate in outside-out patches. This is also the case for crayfish muscle qGluR (Franke and Dudel, 1987). Otherwise, the kinetics of locust muscle qGluR in outside-out patches are very similar to those observed in the intact muscle. In particular, all of the kinetic complexities revealed in our earlier studies (Patlak et al., 1979; Gration et al., 1981*a* and *b*, 1982; Kerry et al., 1987, 1988) remain. We are reasonably confident, therefore, that these complexities are *not* an artifact arising from omission of brief channel events. They have now been seen in (*a*) megaohm studies with a low-pass filter cutoff frequency of $f_c = 1$ kHz (Patlak et al., 1979; Gration et al., 1981*a* and *b*, 1982); (*b*) megaohm studies with $f_c = 3$ kHz (Kerry et al., 1987, 1988); and (*c*) gigaohm studies with $f_c = 10$ kHz. Furthermore, as similar kinetics are seen with cell-attached and excised, outside-out patches,

it seems likely that kinetic state switching is a property of the qGluR per se, and does not reflect a slow modulation of the receptor channel by cytoplasmic events. State switching may be an inherent property of channel proteins. For example, French et al. (1986) described a closely comparable phenomenon when studying batrachotoxin-activated sodium channels reconstituted in lipid bilayers.

Statistical analysis and modeling of qGluR gating kinetics

Analysis of dwell time PDFs and ACFs has allowed us to reveal certain topological features of the qGluR channel gating mechanism. This analysis has been carried out in the context of Markov models (Fitzhugh, 1965; Colquhoun and Hawkes, 1977; Horn, 1984; Fredkin et al., 1985) of the channel gating process. There has recently been some discussion of fractal (Liebovitch and Sullivan, 1987) and of diffusion (Millhauser et al., 1988*a* and *b*; Läuger, 1988) models as alternative descriptions of channel gating. However, as Markov models have been shown to provide superior descriptions of observed channel kinetics for nAChR of rat skeletal muscle, the $GABA_A$ receptor of chick cerebral neurones (McManus et al., 1989*a* and *b*), and for the qGluR of locust muscle (Sansom et al., 1989*b*), we are reassured that their continued use is advisable. In particular, we have addressed the question of the negative correlation between τ_i and α_i values for the qGluR closed time distribution (Table 2). Millhauser et al. (1988*b*) have argued that such a "rate-amplitude correlation" supports a diffusion model of channel gating. We have two reasons for believing that such models do not apply to the qGluR. Firstly, rate-amplitude correlation is not seen for closed time PDFs obtained at low L-glutamate concentrations. Secondly, attempts to fit qGluR open and closed time distributions with PDFs corresponding to diffusion models yielded poorer fits than the Markov model fits described above, as discussed in Sansom et al. (1989*b*).

The dwell time analysis of qGluR gigaohm data suggests that the gating mechanism of the receptor must have $N_o \geq 4$; $N_c \geq 4$; and $N_g \geq 3$. The model ranking arising from preliminary application of maximum likelihood modeling gave models C-4 and C-3 as the best and next best fits to the data. Of the models tested, only C-3 and C-4 satisfied all three of the topological constraints. Thus the two approaches provide comparable results in terms of gating model identification. It is particularly encouraging that the maximum likelihood procedure has been successful, given the relatively modest database employed.

The C-*n* models were chosen for further examination on the basis of our previous experiences of modeling qGluR kinetics using such models, and as a result of our belief that channel gating represents a conformational change of an allosteric protein. The *SC* ranking procedure suggests that the C-4 model is the best descriptor of the qGluR data amongst those models tested. This ranking procedure is similar to that used by Horn and Vandenberg (1984) in their detailed statistical analysis of sodium channel gating. However, there remains a problem in establishing a significance level for the model rankings. The maximum likelihoods ($\hat{L}$) for models C-3 and C-4 are similar. Also, simulations based upon model C-3 yielded a qualitative agreement with the observed channel data, although not as good as that given by the C-4 simulations discussed above. Model C-3 is not a nested subhypothesis of model C-4, and hence it is not possible to use a chi-square test to establish the significance level. Horn (1987) has described a statistical test, based upon the use of simulations, which would in principle allow one to establish whether or not C-4 provides a significantly better fit to the data than C-3. However, this procedure is computationally demanding, and we have established that it would require several months of CPU time using our current maximum likelihood algorithm. We are investigating ways of rendering this approach computationally more feasible.

Overall, we view the C-4 gating models as a reasonable working hypothesis. We need to explore a wider range of models. In particular we wish to seek and test alternative explanations of the state-switching behavior of the qGluR. The C-*n* models generate such behavior by slow agonist association and dissociation. This would be expected to result in a relatively slow activation of the qGluR when exposed to a stepwise increase in L-glutamate concentration. However, recent measurements of the activation kinetics of desensitizing qGluR (Dudel et al., 1988) suggest that such activation is quite rapid. Clearly, other models must be investigated to account for this. Such models are likely to have a larger number of independent parameters, and so a larger experimental database will be required for successful modeling. This in turn will require adaption of the maximum likelihood algorithm to parallel processing architectures so as to reduce CPU times.

APPENDIX

Maximum number of independent parameters obtainable from analysis of time reversible single-channel data

It has been shown by Fredkin et al. (1985) that all the higher order PDFs of a single channel gating mechanism are determined by the

parameters of the second order PDFs:

$$f_{oc}(t, s) = \sum_{i=1}^{N_o} \sum_{j=1}^{N_c} \alpha_{ij} \exp(-\lambda_{it} - \omega_{js}) \quad \text{(A1)}$$

and

$$f_{oc}(s, t) = \sum_{j=1}^{N_c} \sum_{i=1}^{N_o} \beta_{ji} \exp(-\omega_{js} - \lambda_{it}), \quad \text{(A2)}$$

where f_{oc} is the PDF for adjacent open-closed time pairs, (t, s), and f_{co} is the corresponding PDF for closed-open time pairs, (s, t). A single channel gating mechanism at thermodynamic equilibrium is time reversible, i.e., reversing the direction of the time axis does not change the statistical properties of the data. This implies that $f_{oc}(t, s) = f_{co}(s, t)$. As discussed by e.g. Steinberg (1987), this in turn implies that $\alpha_{ij} = \beta_{ji}$. Thus time reversibility implies that all the statistical properties of a single-channel data set are determined by the parameters of $f_{oc}(t, s)$. Counting the number of independent parameters in $f_{oc}(t, s)$, there are N_o values of λ_i, N_c values of ω_j, and N_oN_c values of α_{ij}. However, there is the further constraint that $\Sigma_i \Sigma_j \alpha_{ij} = 1$. *Thus, there are at most* $N_oN_c + N_o + N_c - 1$ *independent parameters.*

Our thanks to Dr. J. Rice (San Diego) for his comments on single channel model identifiability. This work was supported by a grant from the SERC. Dr. Sansom is a Nuffield Foundation Science Research Fellow.

Received for publication 17 October 1989 and in final form 29 March 1990.

REFERENCES

Ball, F. G., and J. A. Rice. 1989. A note on single-channel autocorrelation functions. *Math. Biosci.* 97:1–26.

Ball, F. G., and M. S. P. Sansom. 1988. Single-channel autocorrelation functions: the effects of time interval omission. *Biophys. J.* 53:819–832.

Ball, F. G., and M. S. P. Sansom. 1989. Single channel gating mechanisms: model identification and parameter estimation. *Proc. R. Soc. Lond. B Biol. Sci.* 236:385–416.

Ball, F. G., C. J. Kerry, R. L. Ramsey, M. S. P. Sansom, and P. N. R. Usherwood. 1988. The use of dwell time cross-correlation functions to study single ion channel gating kinetics. *Biophys. J.* 54:309–320.

Bates, S. E., R. L. Ramsey, and P. N. R. Usherwood. 1988. Gigaohm recordings of glutamate-gated channels from adult locust muscle. *Pestic. Sci.* 24:89–90.

Blatz, A. L., and K. L. Magleby. 1989. Adjacent interval analysis distinguishes among gating mechanisms for the fast chloride channel from rat skeletal muscle. *J. Physiol. (Lond.).* 410:561–585.

Clay, J. R., and L. J. DeFelice. 1983. The relationship between membrane excitability and single channel open-close kinetics. *Biophys. J.* 42:151–157.

Colquhoun, D., and A. G. Hawkes. 1977. Relaxation and fluctuations of membrane currents that flow through drug-operated channels. *Proc. R. Soc. Lond. B Biol. Sci.* 199:231–262.

Colquhoun, D., and A. G. Hawkes. 1981. On the stochastic properties of single ion channels. *Proc. R. Soc. Lond. B Biol. Sci.* 211:205–235.

Colquhoun, D., and A. G. Hawkes. 1982. On the stochastic properties of bursts of single ion channel openings and of clusters of bursts. *Phil. Trans. R. Soc. Lond. B.* 300:1–59.

Colquhoun, D., and A. G. Hawkes. 1987. A note on correlations in single ion channel records. *Proc. R. Soc. Lond. B Biol. Sci.* 230:15–52.

Colquhoun, D., and B. Sakmann. 1985. Fast events in single-channel currents activated by acetylcholine and its analogues at the frog muscle end-plate. *J. Physiol. (Lond.).* 369:501–557.

Dudel, J., C. Franke, H. Hatt, R. L. Ramsey, and P. N. R. Usherwood. 1988. Rapid activation and desensitization by glutamate of excitatory, cation-selective channels in locust muscles. *Neurosci. Lett.* 88:33–38.

Efron, B. 1982. The Jackknife, the Bootstrap and other Resampling Plans. Society of Industrial and Applied Mathematics, Philadelphia.

Evans, M., and P. N. R. Usherwood. 1985. The effect of lectins on desensitization of locust muscle glutamate receptors. *Brain Res.* 358:34–39.

Fitzhugh, R. 1965. A kinetic model of the conductance changes in nerve membrane. *J. Cell. Comp. Physiol.* 66:111–118.

Franke, C., and J. Dudel. 1987. Single glutamate-gated synaptic channels at the crayfish neuromuscular junction. I. The effect of enzyme treatment. *Pfluegers Arch. Eur. J. Physiol.* 408:300–306.

Fredkin, D. R., M. Montal, and J. A. Rice. 1985. Identification of aggregated Markovian models: application to the nicotinic acetylcholine receptor. *In* Proceedings of the Berkeley Conference in Honor of Jerzy Neyman and Jack Kiefer. L. M. Le Cam and R. A. Ohlsen, editors. Wadsworth Publishing Co., Belmont, CA. 269–289.

French, R. J., J. F. Worley, M. B. Blaustein, W. O. Romine, K. K. Tam, and B. K. Krueger. 1986. Gating of batrachotoxin-activated sodium channels in lipid bilayers. *In* Ion Channel Reconstitution. C. Miller, editor. Plenum Publishing Corp., New York. 363–383.

Gration, K. A. F., J. J. Lambert, R. L. Ramsey, R. P. Rand, and P. N. R. Usherwood. 1981*a*. Agonist potency determination by patch clamp analysis of single glutamate receptors. *Brain Res.* 230:400–405.

Gration, K. A. F., J. J. Lambert, R. L. Ramsey, and P. N. R. Usherwood. 1981*b*. Nonrandom opening and concentration-dependent lifetimes of glutamate-gated channels in muscle membrane. *Nature (Lond.).* 291:423–425.

Gration, K. A. F., J. J. Lambert, R. L. Ramsey, R. P. Rand, and P. N. R. Usherwood. 1982. Closure of membrane channels gated by glutamate receptors may be a two-step process. *Nature (Lond.)* 295:599–601.

Horn, R. 1984. Gating of channels in nerve and muscle: a stochastic approach. *In* Ion Channels: Molecular and Physiological Aspects. W. D. Stein, editor. Academic Press, Inc., New York. 53–97.

Horn, R. 1987. Statistical methods for model discrimination: applications to gating kinetics and permeation of the acetylcholine receptor channel. *Biophys. J.* 51:255–263.

Horn, R., and K. Lange. 1983. Estimating kinetic constants for single channel data. *Biophys. J.* 43:207–233.

Horn, R., and C. A. Vandenberg. 1984. Statistical properties of single sodium channels. *J. Gen. Physiol.* 84:505–534.

Karlin, A. 1967. On the application of a plausible model of allosteric proteins to the receptor for acetylcholine. *J. Theor. Biol.* 16:306–320.

Kerry, C. J., K. S. Kits, R. L. Ramsey, M. S. P. Sansom, and P. N. R. Usherwood. 1987. Single channel kinetics of a glutamate receptor. *Biophys. J.* 51:137–144.

Kerry, C. J., R. L. Ramsey, M. S. P. Sansom, and P. N. R. Usherwood. 1988. Glutamate receptor-channel kinetics: the effect of glutamate concentration. *Biophys. J.* 53:39–52.

Labarca, P., J. A. Rice, D. R. Fredkin, and M. Montal. 1985. Kinetic analysis of channel gating: application to the cholinergic receptor channel and the chloride channel from *Torpedo californica*. *Biophys. J.* 47:469–478.

Läuger, P. 1988. Internal motions in proteins and gating kinetics of ionic channels. *Biophys. J.* 53:877–884.

Liebovitch, L. S., and J. M. Sullivan. 1987. Fractal analysis of a voltage-dependent potassium channel from cultured mouse hippocampal neurones. *Biophys. J.* 52:979–988.

Mathers, D. A., and P. N. R. Usherwood. 1976. Concanavalin A blocks desensitization of glutamate receptors of locust muscle. *Nature (Lond.)*. 259:409–411.

McManus, O. B., A. L. Blatz, and K. L. Magleby. 1985. Inverse relationship of the durations of adjacent open and shut intervals for Cl and K channels. *Nature (Lond.)*. 317:625–627.

McManus, O. B., A. L. Blatz, and K. L. Magleby. 1987. Sampling, log binning, fitting, and plotting durations of open and shut intervals from single ion channels and the effects of noise. *Pfluegers Arch. Eur. J. Physiol.* 410:530–553.

McManus, O. B., D. S. Weiss, C. E. Spivak, A. L. Blatz, and K. L. Magleby. 1989*a*. Fractal models are inadequate for the kinetics of four different ion channels. *Biophys. J.* 54:859–870.

McManus, O. B., C. E. Spivak, A. L. Blatz, D. S. Weiss, and K. L. Magleby. 1989*b*. Fractal models, Markov models, and channel kinetics. *Biophys. J.* 55:383–385.

Millhauser, G. L., E. E. Salpeter, and R. E. Oswald. 1988*a*. Diffusion models of ion-channel gating and the origin of power-law distributions from single-channel recording. *Proc. Natl. Acad. Sci. USA*. 85:1502–1507.

Millhauser, G. L., E. E. Salpeter, and R. E. Oswald. 1988*b*. Rate-amplitude correlation from single-channel records: a hidden structure in ion channel gating kinetics? *Biophys. J.* 54:1165–1168.

Monod, J., J. Wyman, and J.-P. Changeux. 1965. On the nature of allosteric transitions: a plausible model. *J. Mol. Biol.* 12:88–118.

Ogden, D. C., D. Colquhoun, and C. G. Marshall. 1987. Activation of nicotinic ion channels by acetylcholine analogues. *In* Cellular and Molecular Basis of Cholinergic Function. M. J. Dowdall and J. N. Hawthorne, editors. Ellis Horwood Ltd.,Chichester, UK. 133–151.

Papke, R. L., G. Millhauser, Z. Lieberman, and R. E. Oswald. 1988. Relationships of agonist properties to the single channel kinetics of nicotinic acetylcholine receptors. *Biophys. J.* 53:1–10.

Patlak, J. B., K. A. F. Gration, and P. N. R. Usherwood. 1979. Single glutamate-activated channels in locust muscle. *Nature (Lond.)*. 278: 643–645.

Sansom, M. S. P., F. G. Ball, S. E. Bates, R. L. Ramsey, and P. N. R. Usherwood. 1989*a*. Identification of receptor-channel gating mechanisms: application to a glutamate receptor-channel. *Neurosci. Lett.* 36:S79.

Sansom, M. S. P., F. G. Ball, C. J. Kerry, R. McGee, R. L. Ramsey, and P. N. R. Usherwood. 1989*b*. Markov, fractal, diffusion and related models of ion channel gating: a comparison with experimental data from two ion channels. *Biophys. J.* 56:1229–1243.

Schwarz, G. 1978. Estimating the dimension of a model. *Ann. Stat.* 6:461–464.

Steinberg. I. L. 1987. Frequencies of paired open-closed durations of ion channels: method of evaluation from single-channel recordings. *Biophys. J.* 52:47–55.